Improved compensation networks for dynamic wireless power transfer in a multi-inductor track

Manuele BERTOLUZZO*, Paolo DI BARBA, Michele FORZAN*, Maria Evelina MOGNASCHI**, and Elisabetta SIENI*****

** Dept of Industrial Engineering , University of Padova* , via Gradenigo, 6/a 35131 *Padova, Italy*
E-mail: manuele.bertoluzzo@unipd.it, michele.forzan@unipd.it
*** Dept of Electrical, Computer and Biomedical Engineering , University of Pavia, via Ferrata, 5, 27100 Pavia, Italy*
E-mail: paolo.dibarba@unipv.it eve.mognaschi@unipv.it
****Dept of Theoretical and Applied Sciences, University of Insubria, via Dunant, 3, 21100 Varese, Italy*
E-mail: elisabetta.sieni@uninsubria.it

Purpose – The aim of the paper is to design the compensation network of a dynamic wireless power transfer system, considering the movement of the receiving coil along an electrified track with a large number of inductors buried on the road.

Design/methodology/approach – A Finite Element model has been developed to calculate the self-inductances of transmitting and receiving coils as well as the mutual inductances between the receiving coil and the transmitting ones in the nearby and for various relative positions. The calculated lumped parameters, self-inductances and mutual inductances depending on the relative positions between the coils, have been considered to simulate the compensation network of the active coils, which is composed of three capacitive or inductive reactances T connected. The optimal values of the 6 reactances, 3 for the transmitting coils and 3 for the receiving one, have been calculated by resorting to the Genetic Algorithm NSGA-II.

Findings – In the paper, a broad discussion about the results obtained by means of the optimizations has been done. The optimal values of the reactances of the compensation networks show a clear trend in the receiving part of the circuit. On the other hand, the problem seems very sensitive to the values of the reactances in the transmitting circuit.

Originality/value – Dynamic Wireless Power Transfer System (DWPTS) is one of the newest ways of recharging electric vehicles. Hence, the design of compensation networks for this kind of systems is a new topic and there is the need to investigate possible solutions to obtain a good performance of the recharging system.

Keywords: Finite Element Analysis, Dynamic Wireless Power Transfer. Compensation networks

INTRODUCTION

Dynamic Wireless power transfer systems, DWPTSs, are object of intensive researches since they are expected to enhance the electric vehicle range [1,2]. The first Wireless Power Transfer Systems (WPTSs) were developed as a static recharge station, with the transmitting coil buried in parking area, and intended in substitution of classical plug-in recharger [1,3–5]. The static recharge, already standardized by SAE [5], requires the stop of vehicle in a equipped park area for the time required for battery recharge. Innovative Dynamic systems might allow to recharge the batteries while driving and are the current challenge in vehicle recharge [1,2,6–10].

A Wireless recharge system, both in static and dynamic solution, comprises a receiving coil mounted on the bottom of the vehicle car frame, and one or a set of inductors, the transmitting coils, positioned under the road surface [1,11]. Wireless power transfer systems make use of magnetic induction to transfer the power from the transmitting coil to the receiving coil [2,4,12]. Each coil is equipped with a ferrite layer to concentrate the magnetic flux and to shield the leakage electromagnetic field. The width of the air gap between the coils depends on the vehicle model [5].

The power transferred to the load, i.e. the battery, depends on the compensation network connected to both the transmitting and receiving coil [13–16]. The design of the compensation network aims to improve the power transferred to the load [17,18]. During static recharge the receiving and transmitting coil are in a fixed position that must guarantee a good electromagnetic coupling of the coils, this way the design of the compensation network is relatively easy since the mutual inductance between coils is known and constant. Conversely, in the dynamic recharge of a vehicle the transmitting coils are organized in strip and the mutual inductance varies, depending on the mutual position of the receiving on the transmitting coils [19,20]. This way the mutual inductance experiments a variation during the vehicle movement and the compensation networks have to be designed in order to match different alignment conditions.

In this paper a strip of inductors buried on the road and one receiving coil that shift over the strip are simulated using Finite Element Analysis (FEA) in order to compute the mutual and self-inductance for different reciprocal positions. The obtained mutual and self- inductances were used in the circuital model of the resonant system in order to optimize the compensation networks (CNs) able to guarantee the best performance in the efficiency and power transmission. The considered CNs are formed by three reactive elements arranged in a "T" topology. With a proper selection of their reactances, this layout allows to reproduce the behaviour of most of the CNs considered in the literature [XX]. For this reason, these CNs have been considered in [29], devoted to the optimization of a static WPTS. A dynamic WPTS is analyzed in [YY], where the "T" CNs are optimized considering the receiving coil coupled with only one transmitting coil at a time. The presented paper, instead, considers a dynamic WPTS where the receiving coil is coupled with two transmitting coils at a time, thus representing a much more realistic condition. Moreover, the objective functions (OFs) minimized during the optimization are focused on the average of the efficiency and of the transferred power over different positions, in an attempt to compensate for the variation of the coupling coefficient between the coupled coils while the vehicle moves over the track.

FORWARD PROBLEM

The layout of the DWPT systems consists of a string of transmitting coils (TxCs) buried below the road surface. When a vehicle runs over the track with inductors, the receiving coil, denoted as "pickup coil", is coupled step by step with one or more coils of the track. This arrangement has been studied by means of FEA. The simulated geometry includes 5 TxCs and the pickup, considered perfectly aligned with the main axis of the track [21]. The TxCs and the pickup are identical and composed by 15 turns with an external diameter of 390 mm [22]. The distance between the centres of the TxCs is set to 750 mm. All the coils are equipped with a ferrite layer, a plate with a side of 400 mm and a thickness of 6 mm with an initial relative magnetic permeability of 3000. The model used for the FEA is represented in Fig. 1.

Given the geometry in Fig. 1 FEA solves a time harmonic magnetic field problem using Flux 3D (software released by Altair Engineering[1], Inc. Troy MI, USA[21]). The coils are represented as ideal current windings that act as magnetic field sources and are characterized by absence of discretization (non-meshed coils). the magnetic

[1] https://altairhyperworks.com/product/flux

field produced by the non-meshed coils is evaluated using Biot-Savart formula [23] in a semi-analytical way. In the air volume, the reduced scalar magnetic potential, Φ_R, formulation that takes into account the magnetic field produced by the ideal current paths, is applied while the influence of the ferrite volume is treated by the scalar magnetic potential [24–27]:

$$\nabla \cdot \mu_0 \boldsymbol{H}_s = \nabla \cdot \mu_0 \nabla \Phi_R \tag{3}$$

$$\boldsymbol{H} = \boldsymbol{H}_s - \nabla \Phi_R \tag{4}$$

where $\boldsymbol{H}_s$ is the magnetic field generated by the coil and computed using the Biot-Savart law.

The ferrite volume is described as a continuous strip. The material of the strip is modified according to the position of the coil, and it is air if the coil is not faced on and it acquires the ferrite properties when a coil is faced on a given position [25]. The typical mesh has 344,000 nodes and 1,975,000 first order volume elements.

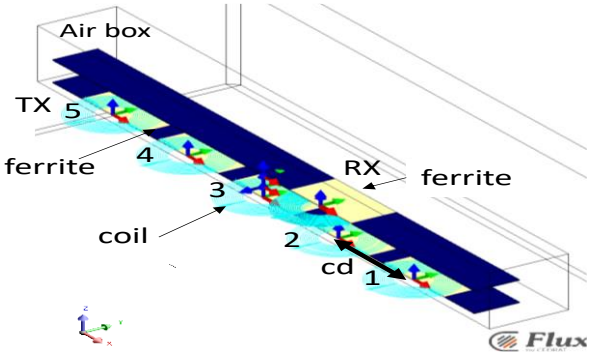

Fig. 1: Layout of the DWPT system model considered for the FEA

FEA is used to evaluate the lumped parameters of the equivalent circuit representing the recharge system. In particular, the self-inductance of the TxCs and pickup have been assessed, and their mutual inductance for different relative positions like in [28].

To this end, the FEA has been performed by supposing that the pickup is supplied with an alternate current having amplitude of 1 A at the frequency f_0=85 kHz [6]. A number of simulations have been performed considering different positions of the pickup, starting from the position A of Fig. 2, centred over the TxC a, and moving on the right with step of 50 mm up to reaching position B, centred on the TxC b. In each position the mutual inductance between the pickup and five TxCs, i.e. coils TxCa, TxCb, TxCc and the ones on the right of "b", TxCd, and on the left of "c", TxCe, have been computed.

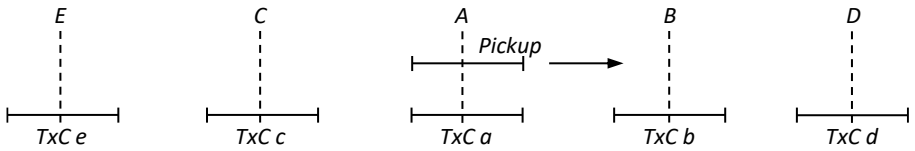

Fig. 2. Pickup positions considered for the FEA.

From the FEA, it resulted that when the pickup is aligned with one of the TxCs, its coupling with the two adjacent ones is about 1% of the coupling existing with the aligned coil. For each position of the pickup coil on the strip of transmitting coils the self and mutual inductances are computed. In particular, Fig. 3 shows the mutual inductance at the terminals of the transmitting coils TxCa and TxCb for different position of the pickup coil. When the pickup coil is aligned to the coil TxCa mutual inductance is maximum at TxCa terminals and minimum at

TxCb terminals and *vice versa*. DESCRIVEFRE COSA SI VEDE IN FIG 3

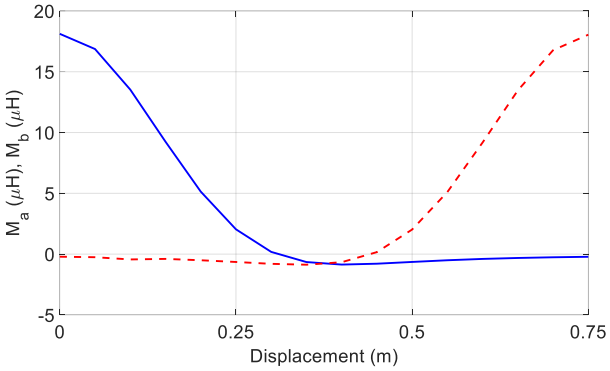

Fig. 3. Mutual inductance M_a (solid blue) and M_b (dashed red) obtained by FEA.

For this reason, the model is accurate even if only two TxCs are considered in the simulation. This condition also entails that in a real system only two coils can be energized at a time, given that there is no advantage in supplying more than two.

OPTIMIZATION PROBLEMS

The performance of a DWPT system is greatly influenced by the compensation networks (CNs) of the coils. The CNs are formed by reactive elements and operate as interfacing circuits between the power supply generator and the TxCs and between the pickup and its equivalent load.

The proposed design considers the pickup equipped with three capacitive or inductive elements and assumes that all the TxCs are connected to equal CNs, each formed by three capacitive or inductive elements. Following from the results of the FEA, the equivalent electrical circuit of the pickup and of the TxCs can be represented as in Fig. 4

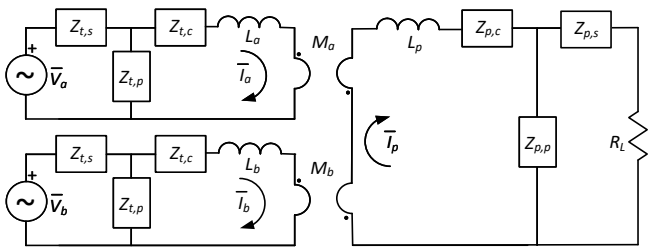

Fig. 4. Equivalent electric circuit of the pickup and of the two coupled TxCs.

In the equivalent circuit, only the two TxCs, which the receiving coil is overlapped to, are considered; the mutual coupling with the other coils can be disregarded. The actual load connected to the CN of the pickup is constituted by the cascade of a rectifier/battery charger and by the battery. All these elements absorb only active energy so that they can be represented by the equivalent resistance R_L.

In order to solve the optimization problem, three Objective Functions (OFs) are formulated as follows:

$$P_{Ls} = \frac{\sum_{i=1}^{\mathrm{Ns}} P_{Li}(x_i)}{\mathrm{Ns}} \tag{1}$$

$$\eta_{\mathrm{a}} = \frac{P_{L,\mathrm{TOT}}}{P_g} \tag{2}$$

$$P\eta = \sum_{i=1}^{\mathrm{Ns}} P_{Li}(x_i) \cdot \eta_i(x_i) \tag{3}$$

where P_{Ls} is the average power on the load, P_{Li} is the power on the load in the x_i position with respect to the transmitting coil strip, N_s is the number of reciprocal positions of the RX-TX coils considered in the computation (e.g. in the example Ns=16), η_{a} is the average efficiency computed as the ratio between the total power supplied to the load, $P_{L,\mathrm{TOT}}$, and the total generated power P_g, $P\eta$ is the product between power and efficiency evaluated as power times the efficiency in each considered position.

Two different optimization problems have been solved: find the values of the 6 reactances of the compensation networks that simultaneously maximize:

1) the average of the power transmitted by the TxCs to the pickup over different positions (OF1) and the average efficiency of the power transmission over different positions (OF2).

2) the average product of the transmitted power times the relevant efficiency over different positions (OF3) and the average efficiency of the power transmission over different positions (OF2).

Problem (1) is focused on the performance of the DWPT system, in terms of transmitted power and efficiency. The first OF in the problem (2) is introduced to avoid solutions with high transmitted power but low efficiency or low transmitted power and high efficiency.

Moreover, the selected CNs must satisfy an additional condition about their impedance at high and low frequency. Both of them must be very high in order to avoid the circulation of any direct current component in the TxCs and to solicitate the DWPT system active and passive elements with undue high frequency current components. To this end, the CNs whose impedances at the frequency $f_0/100$ and/or $f_0 \cdot 100$ are lower than their impedance at f_0 are not considered in the optimization.

OPTIMIZATION ALGORITHM

The design variables of the optimization problem are the six reactances, 3 reactance for the receiving side and 3 for the transmitting side, since the authors hypothesize the same compensation network for all the coils that form the transmitting strip.

In this paper the classical NSGA-II algorithm was used to optimize the two optimization problems 1-2 [29,30]. The population size is 50 individuals and NSGA-II run 200 times to find the Pareto front.

OPTIMIZATION RESULTS

Optimization problem 1)

In this problem, the optimized quantities are the average transmitted power, equation (1), and the average power transmission efficiency, equation (2), both computed considering different positions of the pickup with respect to the TxCs.

The Pareto front obtained by solving the optimization problem 1) is shown in Fig. 5.

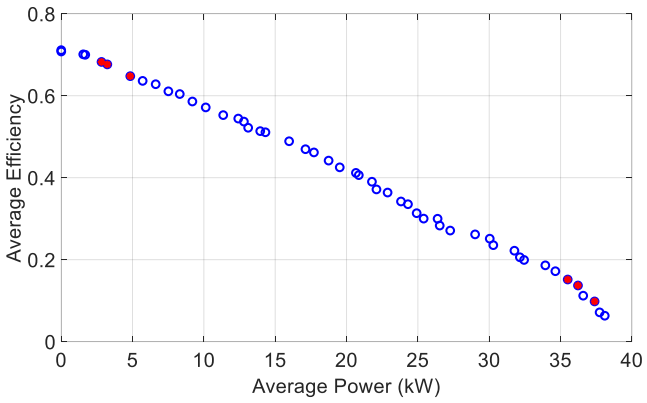

Fig. 5. Pareto from coming from optimization problem (1).

Each of the lines reported in Fig. 6 represents the actual values of the efficiency vs the transferred power achieved in the different positions of the pickup. The circle at the tip of each line highlights the transferred power-efficiency condition relevant to position A (fully-aligned position, see Fig. 2). When the pickup moves toward position B the efficiency and, in most of the cases, the power decreases to zero. This condition is reached when the pickup lays in the middle point between TxCa and TxCb. From this point forward, the efficiency and the power grow again up to coming back to the point highlighted by the circle, this time in correspondence with position B.

The lines relevant to the 50 individuals can be roughly split into two sets by the dashed straight-line. Over this line, the transferred power is nearly maximum in positions A and B. Under this line, the transferred power increases for a while after the pickup leaves position A and grows to the maximum before the pickup reaches position B.

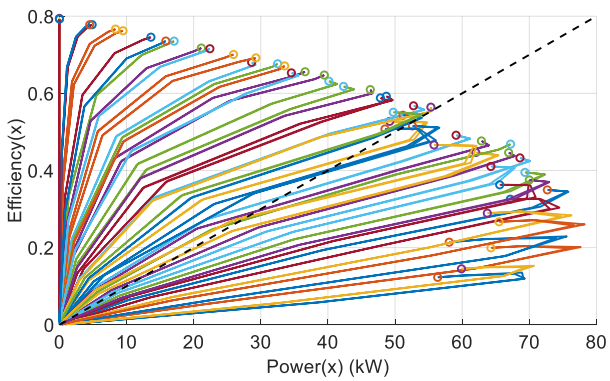

Fig. 6. Efficiency vs. transferred power characteristic of 50 individuals. Each coloured line refers to one point in Fig. 5 and is relevant to the trajectory from A (circle, fully-aligned coils) to B (origin of the axes, fully misaligned coils).

In the following analysis some individuals of each set are considered: three individuals characterized by a transferred power around 10 kW and by a rather high efficiency, highlighted by the red circles in the high-left end of the Pareto front of Fig. 5, and the three individuals that transfer the maximum power at the expenses of a lower efficiency, corresponding to the red circles in the low-right end of the front. These two triplets are denoted as the high efficiency individuals (HEIs) and the high-power individuals (HPIs).

The profiles of the efficiency and of the transferred power for the six selected individuals are reported in Figs. 7. The Fig. 7b highlights the expected condition by which in the three HPIs the maxima of the transferred power do not coincide with position A or position B. This behaviour is similar to that one found when the simple series-series compensation is used and require to reduce the supply voltage of the TxCs whenever the pickup approach them or departs from them in order to avoid any over-solicitation of the DWPT system components.

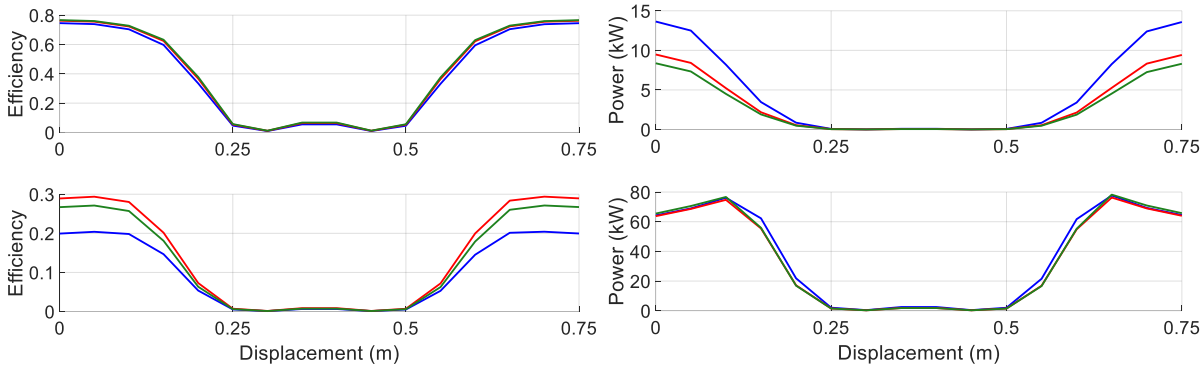

(a) (b)

Fig. 7. (a) Efficiency and (b**)** transferred power of the HEIs (top) and of the HPIs (bottom).

By comparison of the figures, it results that the HEIs and the HPIs exhibit a somehow dual performance: the three HEIs have practically the same efficiency in all the positions of the pickup but transfer different power while the HPIs transfer the same power but with different efficiencies.

The reactances that constitute the CNs of the selected individuals are listed in TableI.

Table I Reactances of the CNs of the TxCx and of the pickup

	HEI_1	HEI_2	HEI_3	HPI_1	HPI_2	HPI_3
$X_{t,s}$	-8.56	-8.44	-8.76	-7.79	-7.64	-7.53
$X_{t,p}$	12.55	12.72	12.69	9.25	9.20	9.06
$X_{t,c}$	-54.79	-60.33	-61.15	-16.95	-22.72	-22.81
$X_{p,s}$	-106.08	-106.00	-105.51	-107.37	-106.44	-107.12
$X_{p,p}$	370.59	370.66	370.37	372.24	372.21	371.53
$X_{p,c}$	45.92	45.88	45.61	44.70	44.10	44.03

In all the considered individuals the reactance $X_{t,s}$ of the CN element $Z_{t,s}$, which is connected in series to the supply system is capacitive, thus assuring that no direct component of current can flow in the circuit.

The reactances of individuals HEI_1 and HPI_1 have been inserted in a circuital simulation developed in the Matlab/Simulik environment to check if the performance relevant to power transfer and efficiency, calculated analytically by the objective functions used for the optimization algorithm, match with those coming from a more

realistic model. In the simulations, a vehicle running at 130 km/h has been considered, so that the time taken to move from the position A to the position B is about 0.021 s.

Fig. 8a is relevant to HEI_1. It shows the profiles of the total power P_s supplied by the supply generator and the power P_L delivered to the equivalent load while the vehicle moves from position A to B and then ahead to the next coil. The solid line plots refer to the simulation results while the dashed line plots refer to the analytical values computed by the objective functions. Fig. 8b shows the power transfer efficiency obtained from the simulation (solid line) and from the objective functions (dashed line). By inspection of the figure, it appears as the matching between the simulation and the analytical results is good enough to be confident in the performance of the objective functions.

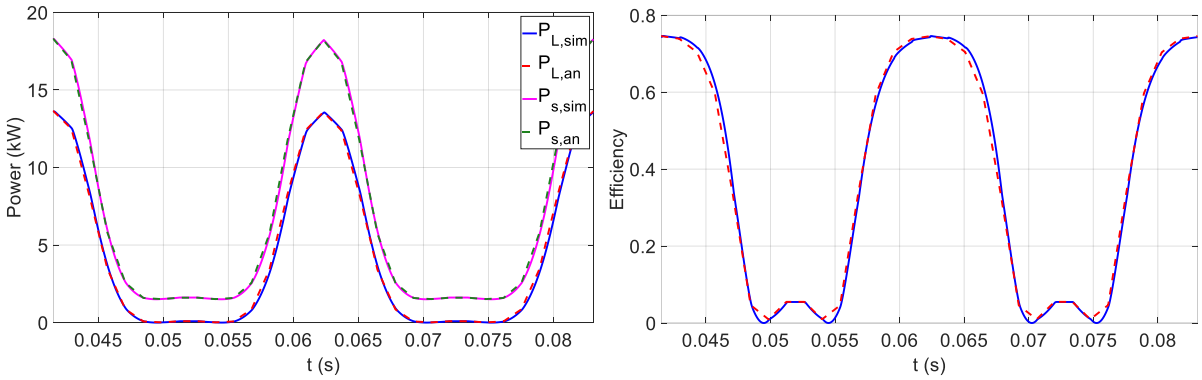

(a) (b)

Fig. 8. (a) Supplied and transferred power and (b) Power transfer efficiency obtained from simulation (blue solid line) and from the objective function (dashed red line).

The same quantities have been computed considering HPE_1. They are plotted in Fig. 9. Also in this case the correspondence between the simulation and analytical results is satisfactory.

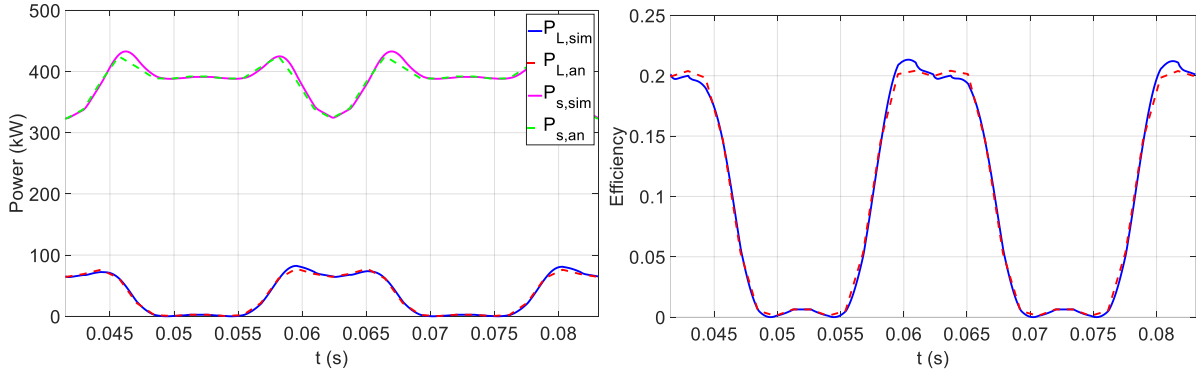

(a) (b)

Fig. 9. (a) Supplied and transferred power and (b) Supplied and transferred power (simulation considers mutual coupling between the TxCs).

The same simulations have been carried out again inserting in the model of the system the mutual inductance existing between the two TxCs, which, depending on the position of the pickup, ranges from about 0.2 μH to 0.4 μH. The obtained results compared whit those coming from the objective functions are reported in the Figs. 10 and 11. The first of them, relevant to HEI_1, demonstrates that the simulation results are nearly equal to those obtained by neglecting the TxCs mutual coupling, so that it can be concluded that the optimized CNs are robust

against its variation. In the case of HPI_1, considered in Fig. 11, the sensitivity of the CNs to the mutual coupling results a little higher, especially when the pickup is not aligned with the TxCs, and this causes an increasing of the supply power and a consequent decreasing of the efficiency. In any case, the results of the simulations are comparable with those coming from the objective functions.

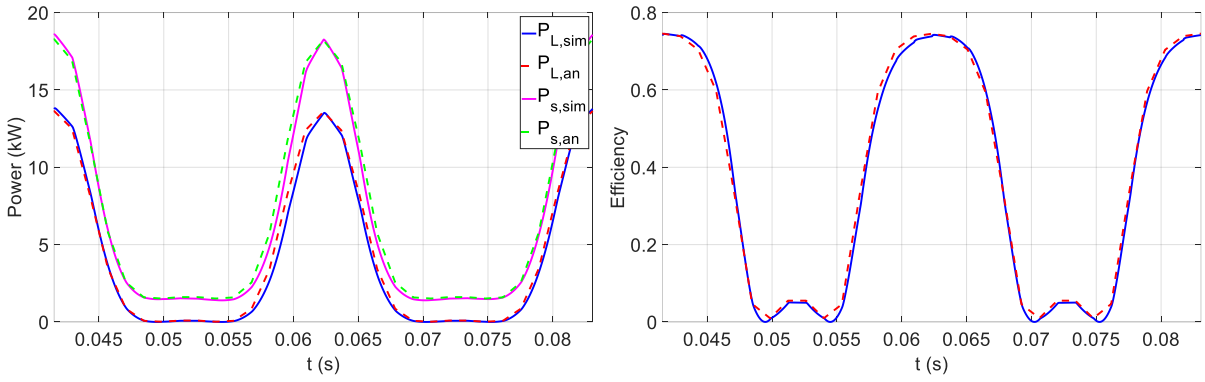

(a) (b)

Fig. 10. Solutions labelled HEI_1: (a) Supplied and transferred power (simulation considers mutual coupling between the TxCs) and (b) Power transfer efficiency obtained from simulation (blue solid line) and from the objective function (dashed red line). Simulation considers mutual coupling between the TxCs.

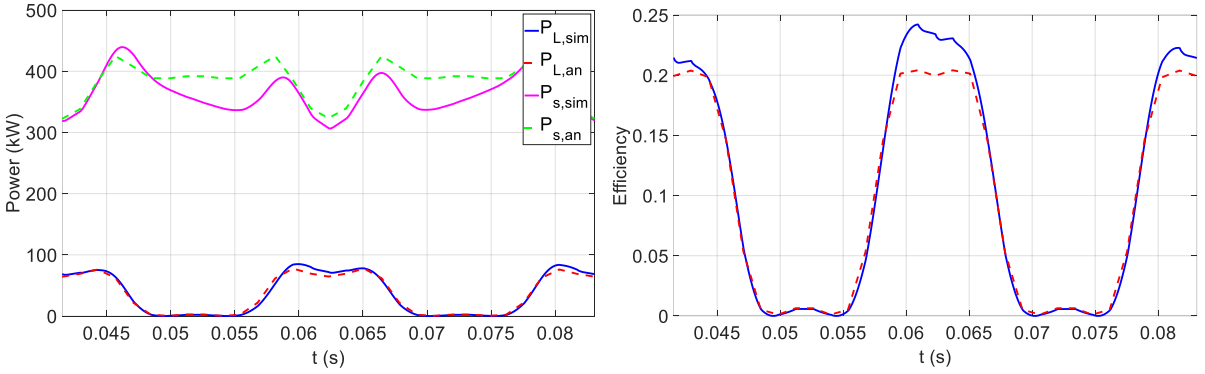

(a) (b)

Fig. 11. Solutions labelled HPI_1: Supplied and transferred power (simulation considers mutual coupling between the TxCs) and (b) Power transfer efficiency obtained from simulation (blue solid line) and from the objective function (dashed red line). Simulation considers mutual coupling between the TxCs).

Optimization problem 2)

In this problem, the optimized quantities are the average product of the transmitted power by the relevant efficiency, equation (3),and the average power transmission efficiency, equation (2), both computed on the different positions of the pickup with respect to the TxCs.

The Pareto front obtained by the solution of the optimization problem 2) is shown in Fig. 12.

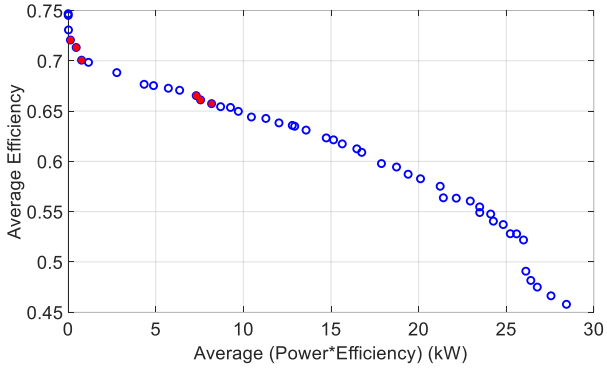

Fig. 12. Pareto front coming from optimization problem (2).

The efficiency as a function of the transferred power in different positions of the pickup is represented in Fig. 13. Also in this case, 50 individuals are considered, each line of Fig. 13 pertaining to one of them.

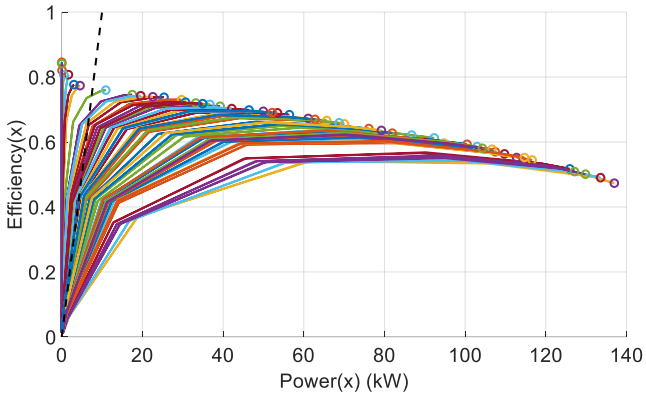

Fig. 13. Efficiency vs. transferred power characteristic of 50 individuals. Each coloured line refers to one point in Fig. 12 and is relevant to the trajectory from A (circle, fully-aligned coils) to B (origin of the axes, fully misaligned coils).

The figure shows that in most of the individuals a comparatively high efficiency is maintained in a rather large power interval while only the few individuals whose power-efficiency characteristics fall on the left of the dashed line exhibit an efficiency constantly increasing with the transferred power. This feature is common in all the individuals obtained by solving the problem 1).

In the following analysis two triplets of individuals have been selected. The first set is characterized by an efficiency higher than 70% but their relevant transferred power is lower than 1 kW. It is highlighted by the red circles in the left-upper end of the Pareto front in Fig. 12 and is denoted as the HEI set. The other set has a little lower efficiency, higher than 65%, but allow to transfer a much higher power that reaches 7.5 kW. These three individuals are positioned about on the first quarter of the Pareto front and are denoted as the HPIs.

The profiles of the efficiency and of the transferred power for the six selected individuals are reported in Fig. 14.

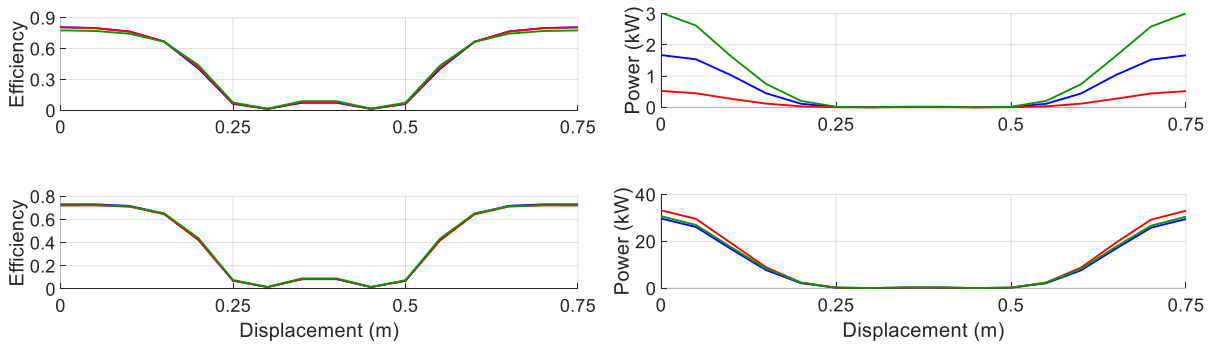

(a) (b)

Fig. 14. (a) Efficiency of the HEIs (top) and of the HPIs (bottom), and (b) Transferred power of the HEIs (top) and of the HPIs (bottom).

Differently from the results coming from Problem 1), now all the individuals reach the maximum transferred power in position A or in position B, where the pickup is aligned with one of the TxCs, whilst in some individuals the maximum efficiency is reached out of these positions.

The optimal reactances that form the CNs of the TxCs and of the pickup are listed in Table II. The CNs of the three HPIs are quite similar one to the other while those relevant to the HEIs have some differences. For both the sets of individuals the reactance $X_{t,c}$, connected in series to the TxC compensates for the self-inductance of the coils itself, thus implementing a series compensation.

Table II Reactances of the CNs of the TxCx and of the pickup

	HEI_1	HEI_2	HEI_3	HPI_1	HPI_2	HPI_3
$X_{t,s}$	-15.35	-32.76	-14.44	-4.24	-3.85	-4.26
$X_{t,p}$	119.66	136.72	15.24	4.64	4.24	4.35
$X_{t,c}$	-65.64	-65.85	-67.05	-64.46	-64.68	-64.64
$X_{p,s}$	-89.56	-91.45	-104.86	-104.43	-106.57	-106.57
$X_{p,p}$	325.23	276.44	332.07	330.06	331.68	331.88
$X_{p,c}$	27.13	30.46	48.29	46.52	49.05	50.37

Simulation have been carried out to check the correspondence between the results coming from the analytical computation of the objective functions and those obtained from a more detailed model of the system that also encompasses the effect of the mutual coupling between the TxCs. As an example, the efficiency and power profiles obtained from the individual HPI_1 are reported in Fig. 15.

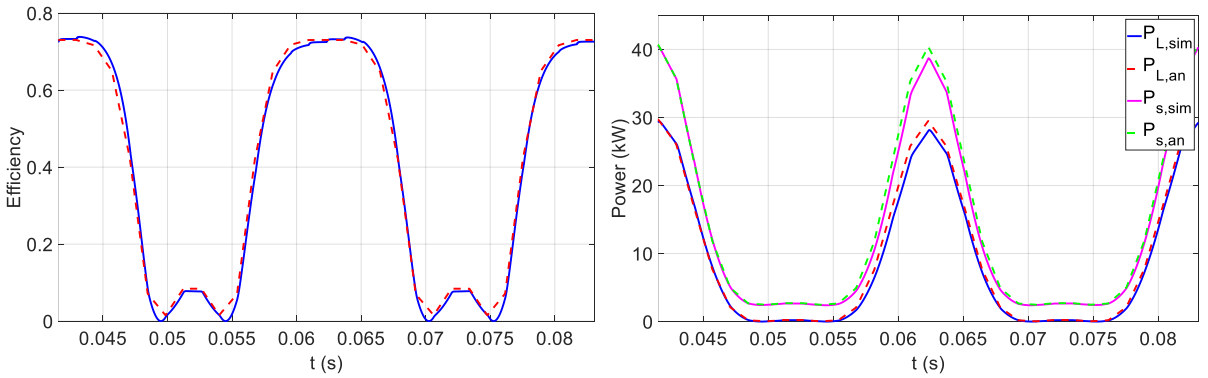

(a) (b)

Fig. 15. Solutions labelled HPI_1: Power transfer efficiency obtained from simulation (blue solid line) and from the objective function (dashed red line). Simulation considers mutual coupling between the TxCs, and (b) Supplied and transferred power (simulation considers mutual coupling between the TxCs).

In both cases there is a good correspondence between the simulation and the analytical results that confirms also in this case the low sensitivity of the CNs to the mutual coupling between the TcCs.

Conclusion

The paper presents the optimization of the CNs of a DWPTS based on a FE model for mutual inductance calculation. The optimal design of the CNs improve the efficiency and transferred power during the electric vehicle movement. This topic is particularly challenging since the pickup coil experiences good alignment and bad alignment conditions periodically. The CNs have to be able to improve the power transfer to the battery guaranteeing feasible conditions. The chosen CNs have to preserve efficiency in aligned condition and avoid too high power, and of an unsuitable value, supplied by the transmitting generator. This paper investigates possible solutions and the most suitable are the ones that improve the efficiency even if they present a power lower than low efficiency solutions. Finally, the power transmitted to the vehicle battery at high efficiency is large enough for practical implementation in the studied device.

REFERENCES

[1] S. Y. Choi, B. W. Gu, S. Y. Jeong, and C. T. Rim, Advances in Wireless Power Transfer Systems for Roadway-Powered Electric Vehicles, *IEEE Journal of Emerging and Selected Topics in Power Electronics*. **3** (2015) 18–36. doi:10.1109/JESTPE.2014.2343674.

[2] Z. Bi, T. Kan, C.C. Mi, Y. Zhang, Z. Zhao, and G.A. Keoleian, A review of wireless power transfer for electric vehicles: Prospects to enhance sustainable mobility, *Applied Energy*. **179** (2016) 413–425. doi:10.1016/j.apenergy.2016.07.003.

[3] S. Lukic, and Z. Pantic, Cutting the Cord: Static and Dynamic Inductive Wireless Charging of Electric Vehicles, *IEEE Electrification Mag.* **1** (2013) 57–64. doi:10.1109/MELE.2013.2273228.

[4] H. Feng, R. Tavakoli, O.C. Onar, and Z. Pantic, Advances in High-Power Wireless Charging Systems: Overview and Design Considerations, *IEEE Trans. Transp. Electrific.* **6** (2020) 886–919. doi:10.1109/TTE.2020.3012543.

[5] J2954_202010 Wireless Power Transfer for Light-Duty Plug-in/Electric Vehicles and Alignment Methodology, (2020). https://www.sae.org/standards/content/j2954_202010/.

[6] L. Tan, M. Zhang, S. Wang, S. Pan, Z. Zhang, J. Li, and X. Huang, The Design and Optimization of a Wireless Power Transfer System Allowing Random Access for Multiple Loads, *Energies*. **12** (2019) 1017. doi:10.3390/en12061017.

[7] D. Bavastro, A. Canova, V. Cirimele, F. Freschi, L. Giaccone, P. Guglielmi, and M. Repetto, Design of Wireless Power Transmission for a Charge While Driving System, *IEEE Transactions on Magnetics*. **50** (2014) 965–968. doi:10.1109/TMAG.2013.2283339.

[8] I. Suh and J. Kim, Electric vehicle on-road dynamic charging system with wireless power transfer technology, in: 2013 International Electric Machines & Drives Conference, 2013: pp. 234–240. doi:10.1109/IEMDC.2013.6556258.

[9] G. Di Capua, A. Maffucci, K. Stoyka, G. Di Mambro, S. Ventre, V. Cirimele, F. Freschi, F. Villone, and N. Femia, Analysis of Dynamic Wireless Power Transfer Systems Based on Behavioral Modeling of Mutual Inductance, *Sustainability*. **13** (2021) 2556. doi:10.3390/su13052556.

[10] G. Di Capua, N. Femia, K. Stoyka, G. Di Mambro, A. Maffucci, S. Ventre, and F. Villone, Mutual Inductance Behavioral Modeling for Wireless Power Transfer System Coils, *IEEE Trans. Ind. Electron.* **68** (2021) 2196–2206. doi:10.1109/TIE.2019.2962432.

[11] S. Li and C. C. Mi, Wireless Power Transfer for Electric Vehicle Applications, *IEEE Journal of Emerging and Selected Topics in Power Electronics*. **3** (2015) 4–17. doi:10.1109/JESTPE.2014.2319453.

[12] L. Sun, D. Ma, and H. Tang, A review of recent trends in wireless power transfer technology and its applications in electric vehicle wireless charging, *Renewable and Sustainable Energy Reviews*. **91** (2018) 490–503. doi:10.1016/j.rser.2018.04.016.

[13] Z. Zhou, L. Zhang, Z. Liu, Q. Chen, R. Long, and H. Su, Model Predictive Control for the Receiving-Side DC–DC Converter of Dynamic Wireless Power Transfer, *IEEE Trans. Power Electron.* **35** (2020) 8985–8997. doi:10.1109/TPEL.2020.2969996.

[14] H.K. Dashora, G. Buja, M. Bertoluzzo, R. Pinto, and V. Lopresto, Analysis and design of DD coupler for dynamic wireless charging of electric vehicles, *Journal of Electromagnetic Waves and Applications*. **32** (2018) 170–189. doi:10.1080/09205071.2017.1373036.

[15] W. Chen, W. Lu, H.H.-C. Iu, and T. Fernando, Compensation Network Optimal Design Based on Evolutionary Algorithm for Inductive Power Transfer System, *IEEE Trans. Circuits Syst. I.* **67** (2020) 5664–5674. doi:10.1109/TCSI.2020.3012700.

[16] W. Zhang, and C.C. Mi, Compensation Topologies of High-Power Wireless Power Transfer Systems, *IEEE Trans. Veh. Technol.* **65** (2016) 4768–4778. doi:10.1109/TVT.2015.2454292.

[17] A. Ali, M.I. Sulaiman, M.N.M. Yasin, M.M. Azizan, M. Jusoh, N.A.M.A. Hambali, and M.H. Mat, Wireless power transfer (WPT) optimization using resonant coil, in: Strbske Pleso, Slovak Republic, 2019: p. 020127. doi:10.1063/1.5118135.

[18] W. Zhang and C. C. Mi, Compensation Topologies of High-Power Wireless Power Transfer Systems, *IEEE Transactions on Vehicular Technology*. **65** (2016) 4768–4778. doi:10.1109/TVT.2015.2454292.

[19] S. Barmada, A. Musolino, J. Zhu, and S. Yang, A Novel Coil Architecture for Interoperability and Tolerance to Misalignment in Electric Vehicle WPT, *IEEE Trans. Magn.* **59** (2023) 1–5. doi:10.1109/TMAG.2023.3235713.

[20] L. Sandrolini, M. Simonazzi, S. Barmada, and N. Fontana, Two-port network compact representation of resonator arrays for wireless power transfer with variable receiver position, *Circuit Theory & Apps*. **51** (2023) 2301–2314. doi:10.1002/cta.3510.

[21] FLUX, (Altair): https://altairhyperworks.com/product/flux, (n.d.).

[22] G. Buja, M. Bertoluzzo, and K.N. Mude, Design and Experimentation of WPT Charger for Electric City Car, *IEEE Trans. Ind. Electron.* **62** (2015) 7436–7447. doi:10.1109/TIE.2015.2455524.

[23] P. Ferrouillat, C. Guerin, G. Meunier, B. Ramdane, P. Labie, and D. Dupuy, Computations of Source for Non-Meshed Coils With A–${V}$ Formulation Using Edge Elements, *IEEE Trans. Magn.* **51** (2015) 1–4. doi:10.1109/TMAG.2014.2365293.
[24] G. Meunier, ed., The finite element method for electromagnetic modeling, ISTE ; Wiley, London : Hoboken, NJ, 2008.
[25] F. Dughiero, M. Forzan, C. Pozza, and E. Sieni, A Translational Coupled Electromagnetic and Thermal Innovative Model for Induction Welding of Tubes, *IEEE Transactions on Magnetics*. **48** (2012) 483–486. doi:10.1109/TMAG.2011.2174972.
[26] K.J. Binns, P.J. Lawrenson, and C.W. Trowbridge, The analytical and numerical solution of electric and magnetic fields, Wiley, Chichester, 1992.
[27] Dughiero F., M. Forzan, and Sieni E., Simple 3D fem models for evaluation of EM exposure produced by welding equipments, in: Studies in Applied Electromagnetics and Mechanics, Ios Pr Inc, 2010: pp. 911–919.
[28] M. Bertoluzzo, P. Di Barba, M. Forzan, M.E. Mognaschi, and E. Sieni, Wireless Power Transfer System in Dynamic Conditions: A Field-Circuit Analysis, *Vehicles*. **4** (2022) 234–242. doi:10.3390/vehicles4010015.
[29] M. Bertoluzzo, P. Di Barba, M. Forzan, M.E. Mognaschi, and E. Sieni, Multiobjective optimization of compensation networks for wireless power transfer systems, *COMPEL*. **41** (2022) 674–689. doi:10.1108/COMPEL-06-2021-0204.
[30] K. Deb, A. Pratap, S. Agarwal, and T. Meyarivan, A fast and elitist multiobjective genetic algorithm: NSGA-II, *Evolutionary Computation, IEEE Transactions on DOI - 10.1109/4235.996017*. **6** (2002) 182–197.